

Heat Pumps in Battery-Electric Agricultural Machinery for the Utilisation of Waste Heat

Benjamin Wilk, Jan Wieckhorst, Philipp Heymann, Ludger Frerichs

This paper investigates the potential of heat pumps with secondary circuits for utilising waste heat in battery-electric agricultural machinery, as well as their impact on the machine's operational duration, particularly regarding the heating of the vehicle cabin and traction battery. A compact R134a heat pump system with a water-glycol secondary circuit is constructed on a test bench, characterised through measurements, and balanced regarding temperatures, pressures, and volume flows. From the measurement data, coefficients of performance (COP) and thermal outputs are derived and processed via k-Nearest Neighbours interpolation (k-NN) into lookup tables based on evaporator and condenser inlet temperatures for a 0D/1D simulation. On this basis, a 100 kW/100 kWh tractor is analysed, and the heat pump is compared to a resistive heater in realistic operating scenarios. The study thereby reveals potential and limitations of waste heat utilisation and derives implications for design, integration, and operation of future thermal management systems in electrified agricultural machinery.

Keywords

Thermal management system, heat pump, agricultural tractor, battery-electric tractor

In contrast to vehicles with internal combustion engines, where the range issue is hardly relevant due to the high energy density of liquid fuels, electromobility in the agricultural and construction machinery sector presents new challenges. In combustion engines, the abundant waste heat is used to heat the passenger compartment. Battery-electric vehicles, on the other hand, generate only limited waste heat, which means that conventional heating concepts based on resistive heating in these vehicles can lead to reductions in both range and service life. Therefore, the electrification of the agricultural and construction machinery sector requires innovative solutions with high energy efficiency to minimize these limitations (PRAETORIUS 2018, MARKETS and MARKETS 2025). In the passenger car sector, measures such as infrared-reflective glazing, heat pumps, and waste heat recovery in interior ventilation achieve range advantages of approximately 10–30% (SUCK and SPENGLER 2014). In the field of battery-electric tractors, the use of a heat pump system for cabin heating as well as battery conditioning was demonstrated in a development vehicle presented by FENDT in 2017 (BREU and PICHLMAIER 2017), however, this concept has not yet been implemented in series production vehicles (AGCO GMBH 2026). By comparison, the Rigitrac SKE 40 series vehicle is equipped with an integrated heat pump system. Additionally, the option of heat recovery at low temperatures is mentioned, although it remains unclear whether the waste heat is used solely within the heat pump system or can also be used directly (AGROFOSSILFREE 2020, RIGITRAC TRAKTORENBAU AG 2025). Heat pumps represent a promising alternative to conventional resistive heating for electrified agricultural machinery because they utilize waste heat from electrical components such as the electric motor,

inverter, and drivetrain. The focus of this work is on the analysis of heat pump systems with secondary circuits, as extensively described by WEUSTENFELD (2018) for battery-electric vehicles, as well as on a comparison with conventional resistive heating.

Heat pump test bench

To determine the specific characteristics of a heat pump, a cold vapor process with a water-glycol secondary circuit is set up. The system is equipped with sensors that measure the temperature and flow rate of the heat exchangers under investigation. Additionally, combined pressure and temperature sensors are installed in the cold vapor process. These sensors are necessary for controlling the electronic expansion valve as well as the refrigerant compressor. Furthermore, the refrigerant pressure and temperature values recorded at the measurement points provide important information for calculating the internal thermal performance (DOHMANN 2016). The heat pump system is compactly integrated into a common frame, which, in addition to the heat exchangers, also includes the high-voltage heater and the pumps (Figure 1).

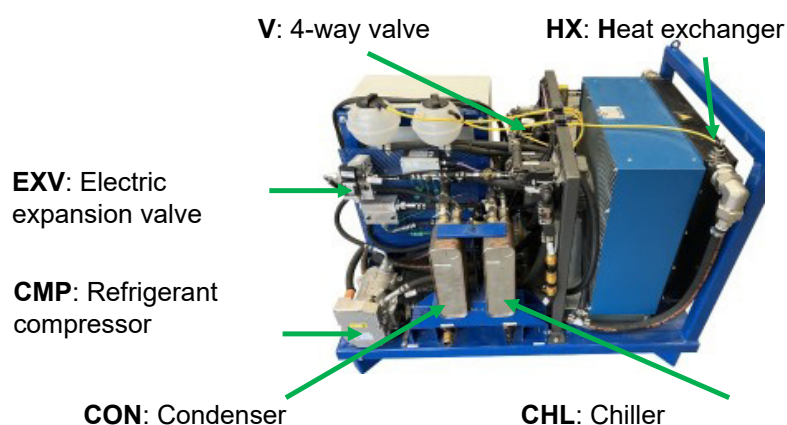


Figure 1: Layout and components of the heat pump test bench

Figure 2 illustrates the schematic system layout for heat pump operation and the corresponding sensor placement for measuring characteristic system parameters. Especially important are measurements of volume flow and temperature differences across the plate heat exchangers CHL (evaporator) and CON (condenser). The electrical power consumed by the refrigerant compressor (CMP) is drawn from the power supply. The COP (Coefficient of Performance) is calculated as the ratio of generated thermal power to electrical input power (Joos 2004).

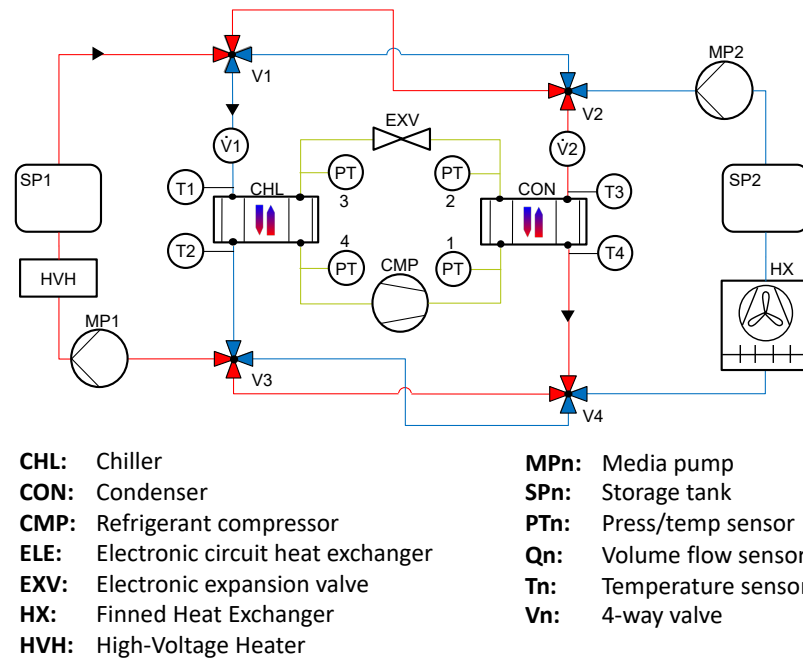


Figure 2: System diagram for heat pump operation of the test bench; red = secondary circuit of refrigerant condenser, blue = secondary circuit of refrigerant evaporator; triangle = flow direction

Figure 3 shows the system state during refrigeration operation. The valves V1-V4 are switched so that cooled heat transfer fluid arrives in the storage tank SP1 from the evaporator. The temperature in the tank drops until the refrigerant mass flow can no longer be fully evaporated in the evaporator. To protect against liquid slugging in the refrigerant compressor, the system operation is stopped at this operating point.

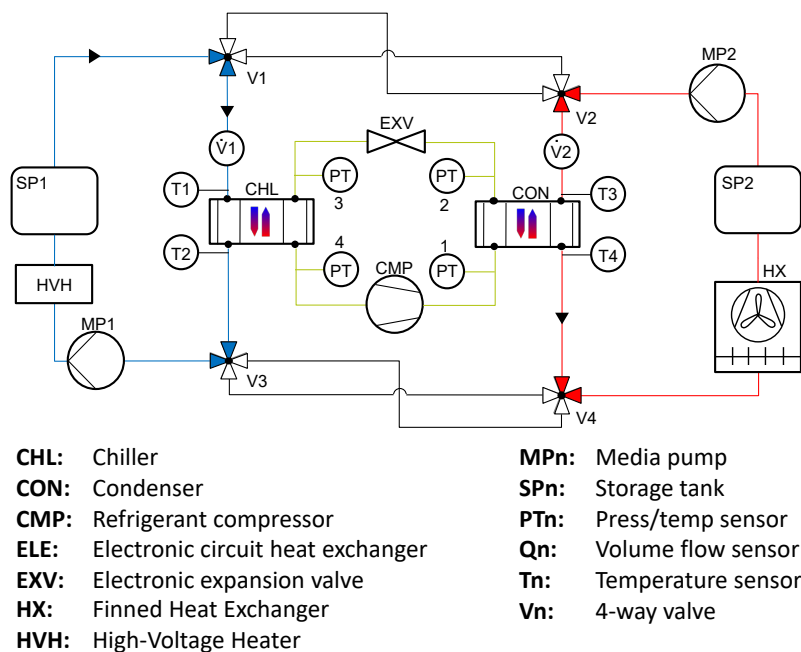


Figure 3: System layout for refrigeration operation of the test bench; red = secondary circuit of refrigerant condenser, blue = secondary circuit of refrigerant evaporator, triangle = flow direction

Table 1 presents an exemplary data set for heat pump operation at three different refrigerant compressor speeds (n in 1/min). Measured values include inlet and outlet temperatures of the heat exchanger on the cold side ($T1, T2$) and the warm side ($T3, T4$), coolant volume flow (V and $\dot{V}2$) in litres per minute, thermal power ($\dot{Q}1$ and $\dot{Q}2$) in kilowatts, electrical compressor power consumption (P) in kilowatts, and the calculated COP. The data demonstrate how thermal power and efficiency vary with increasing compressor speed and temperature conditions. For instance, at constant speed, increasing cold-side temperature ($T1$) leads to higher heat output ($\dot{Q}2$) on the warm side and an improved COP.

Table 1: Example of a measurement dataset for heat pump operation with three different refrigerant compressor speeds. Heat output (positive), heat input (negative)

n in 1/min	$T1$ in °C	$T2$ in °C	$\dot{V}1$ in l/min	$\dot{Q}1$ in kW	$T3$ in °C	$T4$ in °C	$\dot{V}2$ in l/min	$\dot{Q}2$ in kW	P in kW	COP
2500	6	4.7	17.5	-1.35	44.3	46.9	20	3.08	1.8	1.61
2500	10	8.4	17.5	-1.66	47.7	50.8	20	3.68	2.0	1.73
2500	15	12.6	17.5	-2.49	49.4	53.4	20	4.74	2.2	2.03
3500	5	4.1	18.6	-0.99	45.1	47.3	23	3.00	2.4	1.18
...
5000	15	12.2	19.5	-3.24	56	61.1	24	7.26	5.1	1.34

The lookup table in Table 2 enables the determination of the generated thermal power, which is defined at each operating point and can be assigned to an electrical refrigerant compressor power. The data from Table 1 are interpolated using the k-NN method and plotted in the lookup table with a constant step size for the evaporator and condenser inlet temperatures (ERTEL 2025). Each lookup table corresponds to a fixed coolant volumetric flow rate in both coolant circuits and a fixed refrigerant compressor speed.

Table 2: Evaporator performance table $\dot{Q}2$ in kW for a refrigerant compressor speed of $n = 2500$ 1/min and a coolant volumetric flow rate of $\dot{V}1 = 20$ l/min with variation of the evaporator inlet temperature ($T1$) and the condenser inlet temperature ($T3$)

		$T1$ in °C				
		29.5	29.6	29.7	...	49.4
$T3$ in °C	6	5.3	5.3	5.2	...	2.2
	6.3	5.3	5.3	5.2	...	2.2
	6.6	5.3	5.3	5.3	...	2.2

	70	6.4	6.4	6.5	...	6.7

If the evaporator capacity is to be provided for different compressor speeds or refrigerant volumetric flow rates, a separate lookup table must be created for each operating point. The described measurement data and lookup tables form the basis for a numerical simulation of the heat pump operation. By using the k-NN method, continuous characteristic curves can be generated from discrete measurement points, which represent the behaviour of the heat pump in a simulation under varying inlet and outlet temperatures as well as varying compressor speeds and refrigerant volumetric flow rates. For each defined operating point, the producible thermal capacities and electrical power con-

sumption are determined using the lookup tables. From this, the COP is derived, characterizing the efficiency of the system under the respective operating conditions.

By simulating over a time course with varying environmental conditions, the dynamic performance and efficiency of the heat pump system can thus be predicted. Moreover, the computational effort of the simulation is low because no complex calculations are required to determine efficiency and performance within the framework of a two-phase process.

Thermal efficiency and temperature limits

The COP is the ratio of produced heat to input electrical energy. A COP of 3 means 3 kWh of heat are generated per 1 kWh electrical energy consumed. Measurements on an R134a heat pump with secondary circuit revealed an overall COP exceeding four at the optimum point (Figure 4).

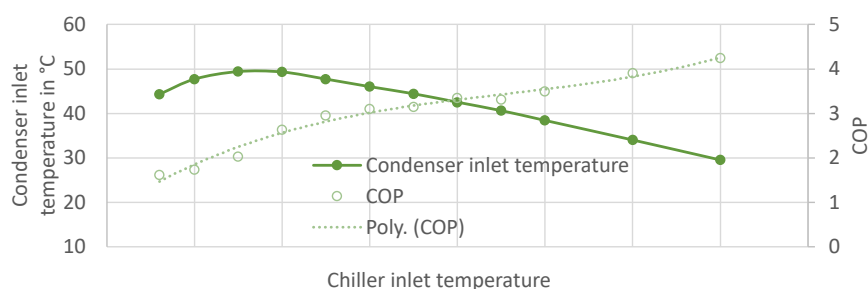


Figure 4: Coefficient of Performance of an R134a heat pump with secondary circuit (KORFF 2024)

Heat pumps exhibit a higher efficiency compared to resistive heating systems, which typically have a COP of 1. In particular, the utilization of waste heat from the secondary circuit can further increase efficiency, if available in sufficient quantities. For a quantitative comparison of heating system architectures, the temperature-dependent usable battery capacity must also be considered. Figure 5 shows the temperature-dependent discharge curves of the battery cell. At a cell temperature of 0 °C, the end-of-discharge voltage is reached after extracting about 85% of the capacity available at 20 °C, whereas at 20 °C the entire capacity (nominal capacity) of the battery cell is usable (DOPPELBAUER 2025). The Depth of Discharge (DOD) describes the ratio between the extracted charge and the nominal capacity. However, for assessing machine usage duration, the usable energy is decisive, which is determined by the integral of the voltage over the extracted capacity. Since the voltage curve at 0 °C runs overall at a lower level, a reduction in the DOD by 15% does not necessarily correspond to a proportional decrease in usable energy. The order of magnitude is comparable, however, so this assumption is used for the following estimates.

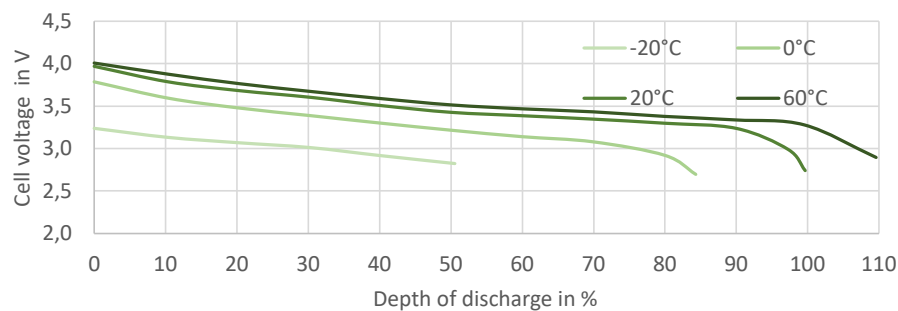


Figure 5: Cell voltage over discharged energy at different ambient temperatures (DOPPELBAUER 2025)

An important aspect when utilizing waste heat is the temperature limit of the available heat sources. In cold environments (low evaporator inlet temperatures and high condenser outlet temperatures), the efficiency of the heat pump can decrease, involving a hybrid solution with additional heating methods. For this purpose, a resistance heater is used at low temperatures to heat the cabin and the battery. However, not only low evaporator inlet temperatures but also high inlet temperatures offer challenges. At high evaporator inlet temperatures, the electric compressor may fail because the compressed refrigerant can reach temperatures well above 100 °C. Commercially available electric refrigerant compressors shut down when a temperature is exceeded to protect themselves from damage. The maximum temperature limit depends on the refrigerant compressor used.

Secondary circuit for waste heat utilisation

Figure 6 shows a possible thermal management system (TMS) that couple's multiple subsystems via plate heat exchangers. At the centre of the setup is the thermodynamic cycle of the heat pump (in subsystem A), which is connected to the other subsystems through the secondary circuit. The plate heat exchangers ELE and GBX couple the circuits of the electrical components (subsystem D) and the drivetrain (subsystem C) to the secondary circuit of the heat pump. This allows the waste heat generated there to be used as a heat source for the heat pump cycle and to provide heating for other components. The battery conditioning circuit (subsystem B) is integrated into the overall system via the plate heat exchanger BAT. Thus, depending on the operating condition, the battery can be both heated and cooled. For this reason, fully coupled system architecture enables efficient thermal integration of all main heat sources and sinks. It allows demand-oriented temperature control of all subsystems. The possible operating states of the TMS include various heating and cooling functions for the vehicle components. The optimal temperature range for the battery is between 25 and 30 °C. The possible TMS functions, with the shown setup, are generally defined as follows:

- Cool battery using refrigeration system: The battery is actively cooled with a refrigeration system to ensure optimal operating temperatures.
- Cool battery to ambient: Heat is directly released to the ambient environment to lower the battery temperature.
- Heat battery with high-voltage heater: The high-voltage heater warms the battery at low outside temperatures.
- Heat battery with heat pump: The heat pump uses thermal energy (waste heat flow) to efficiently warm the battery.
- Heat battery with waste heat: Direct waste heat utilization from other components serves to heat the battery.

- Cool cabin with refrigeration system: The vehicle cabin is cooled using a refrigeration system.
- Heat cabin with high-voltage heater: The high-voltage heater provides rapid and targeted heating of the vehicle cabin.
- Heat cabin with heat pump: The heat pump uses thermal energy (waste heat flow) to efficiently warm the vehicle cabin.
- Heat cabin with waste heat: Waste heat from the system is used to heat the cabin (as known from combustion engine vehicles).
- Cool oil to ambient: The lubrication and hydraulic oil is maintained at an optimal temperature by releasing heat to the ambient environment (via HX3/HX1).
- Cool electronics to ambient: Electronic components are actively cooled by releasing heat to the ambient environment (via HX1).

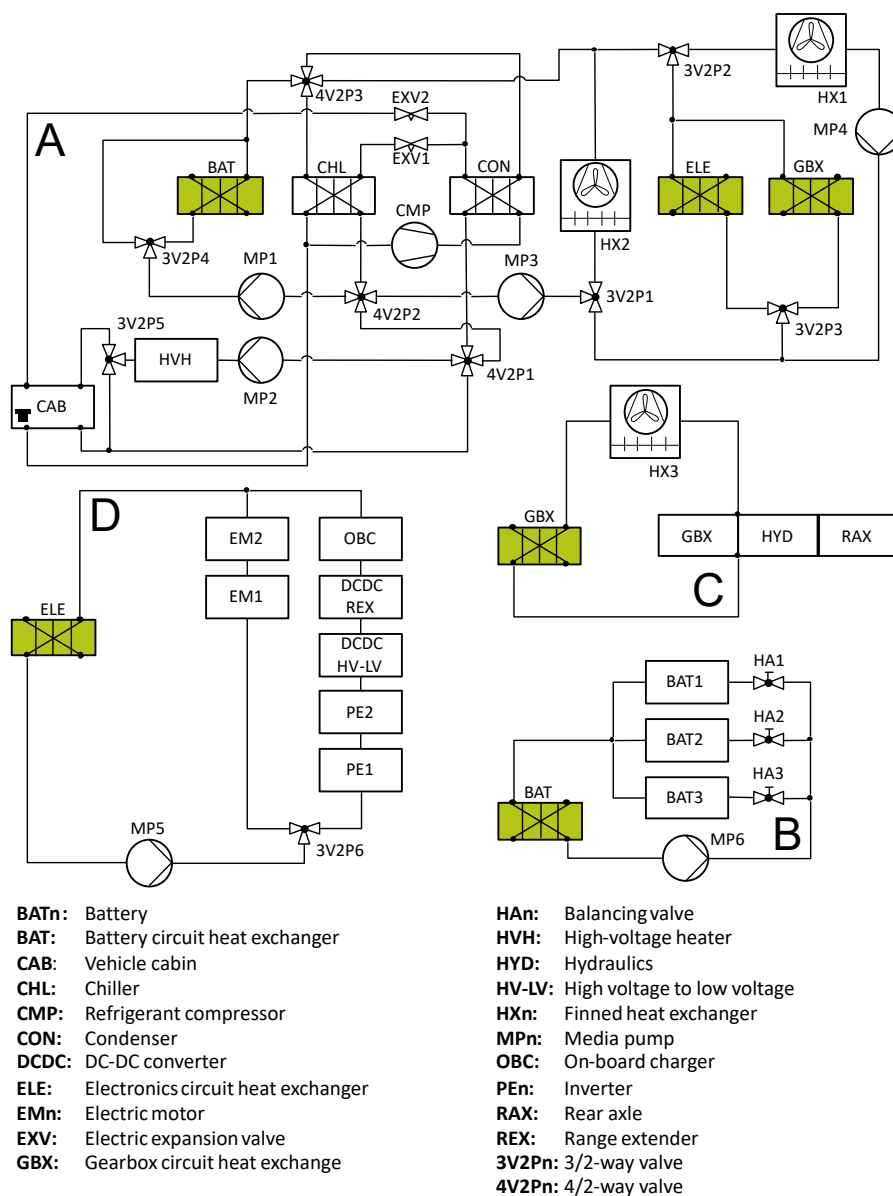


Figure 6: Layout of a thermal management system for a battery-electric agricultural machine

Comparison of machine operational duration using two heating methods

An electrified tractor is considered as the base vehicle. Based on the typical usage profile, the potential for energy savings using a heat pump will be demonstrated in the further course of this work. To classify the vehicle power class and energy storage size, a maximum power of 100 kW with a usable energy storage capacity of 100 kWh is assumed for the following investigations. For better illustration of the application scenarios and machine utilization, Figure 7 exemplarily shows the utilization of a battery-electric tractor depending on the work to be performed.

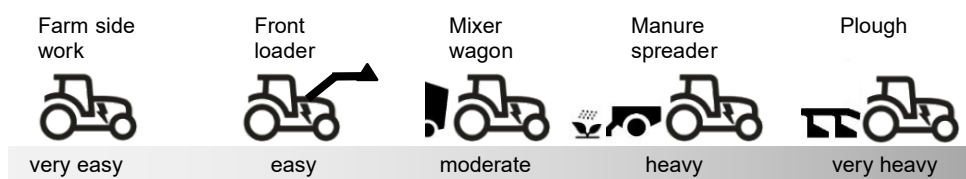


Figure 7: Machine utilization based on a tractor

The comparison example in Figure 8 illustrates various operating scenarios for a tractor. In this case, the vehicle is started cold at 0 °C, and both the battery and cabin are heated to 20 °C. The comparison shows the potential extension of the maximum machine operating time when the vehicle is heated using a heat pump with different COP values, compared to resistance heating. Since the heating process starts at 0 °C, a usable battery capacity of 85% is assumed. Under light machine load, savings of approximately 7% at a COP of 2 and up to 11% at a COP of 4 can be achieved (Figure 8, left chart). The right chart in Figure 8 further illustrates the possible extension of machine operating time in minutes for better understanding. Under light machine workload, the extension can range from 14 to 22 minutes. The maximum total operating time of the tractor is thus 3.3 hours.

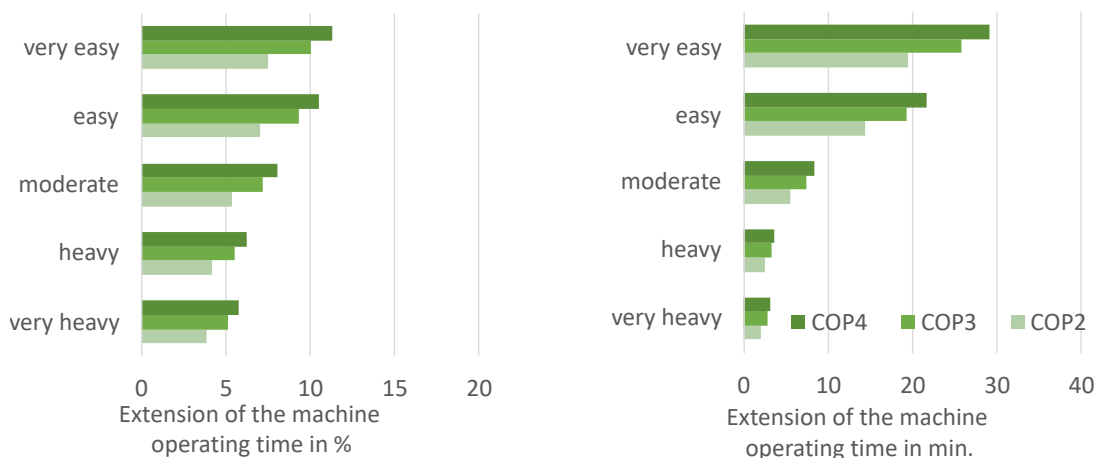


Figure 8: Comparison of machine operating time between heat pump and resistance heating in the case of a cold start, COP: Coefficient of Performance

Figure 9 illustrates the machine operating time of the tractor at a starting temperature of 0 °C and a usable battery capacity of 85%. Various scenarios are shown with and without heating of the vehicle components (cabin and battery). The bottom group of bars represents the reference case without heating, achieving a maximum operating time of over 4.3 hours. The use of a high-voltage heater

(HVH), which corresponds to a COP of approximately 1 due to its efficiency, significantly reduces the operating time because a substantial portion of the electrical energy must be consumed for heat generation. As the COP increases, meaning a higher efficiency of heat generation (using a heat pump), the possible operating time extends again.

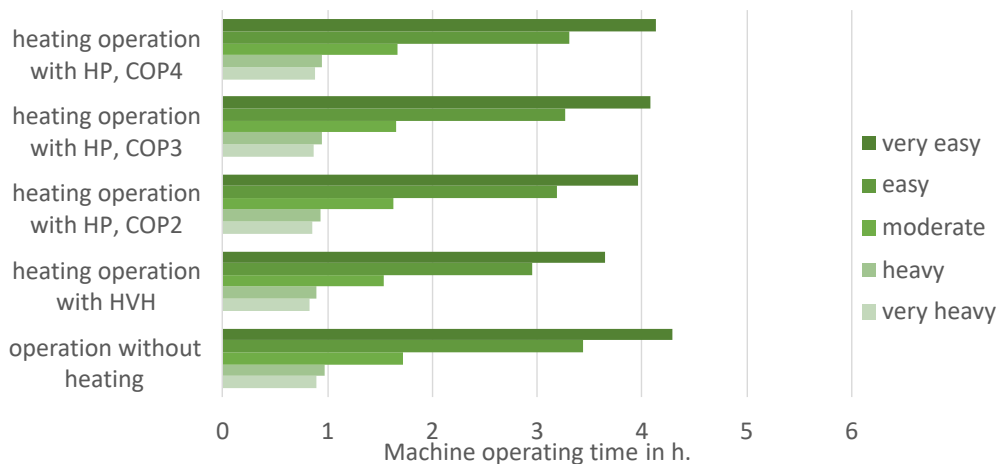


Figure 9: Machine operating time with variations in heating and machine load; battery 85% DOD, HVH = high-voltage heater, HP = heat pump, COP = Coefficient of Performance

With a COP of 4, the machine operating time comes very close to the reference scenario without heating. It is noticeable that the potential for extending the machine operating time increases as the machine load decreases. The reason for this is the constant heating demand of the cabin, which never fully disappears at an ambient temperature of 0 °C. At low machine loads, this constant heat flow represents a larger proportion of the total energy consumption, making efficiency improvements in the heating system more significant.

Figure 10 presents various operating scenarios for a tractor with a preheated system (cabin and battery). In this case, the machine is started cold at an outside temperature of 0 °C, while the battery and cabin are preheated to 20 °C (warm start). The electrical energy for this is drawn from the power grid and not from the battery. Additionally, due to the preconditioning of the battery via the power grid, its full capacity is usable. The comparison shows that at low loads, the extension of the machine operating time is reduced to about 2.6% at a COP of 2 and to 3.9% at a COP of 4. The extension of the machine operating time is then 6 to 10 minutes, resulting in a total operating time of approximately 4 hours.

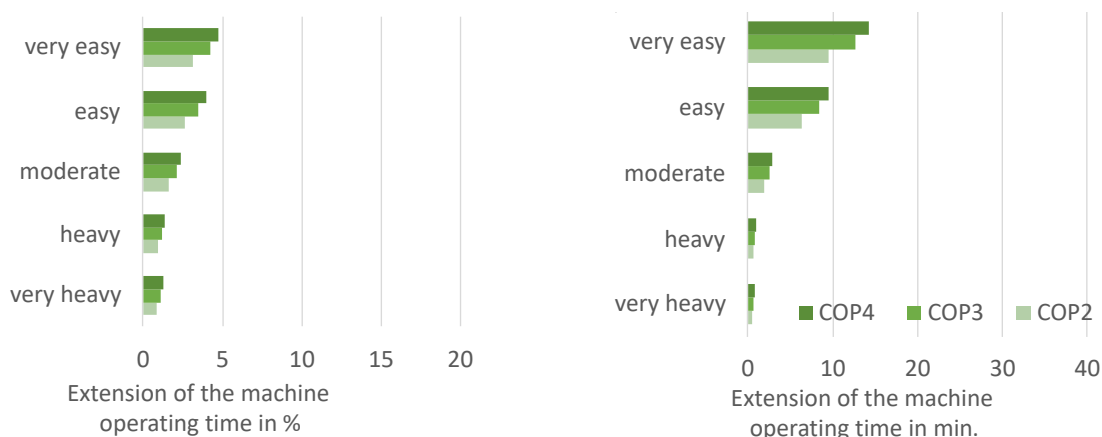


Figure 10: Comparison of machine operating time between heat pump and resistance heating in the case of a warm start, COP = Coefficient of Performance

Figure 11 illustrates that with 100% usable battery capacity (preheated battery and cabin) and very light load, a machine operating time of 5 hours is achieved. Due to the preconditioning of the battery and cabin, which takes about 30 minutes and requires approximately 4.75 kWh of energy, these components no longer need to be heated during operation but only maintained at temperature. As a result, the heat demand for heating during the machine operating time is low. Consequently, the machine operating time changes only marginally at a COP of 4.

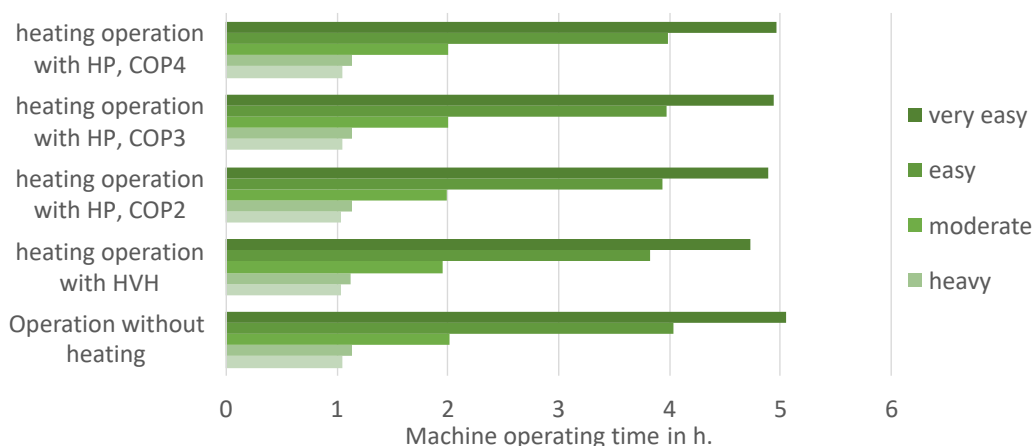


Figure 11: Machine operating time with variations in heating and machine load; battery 100% DOD, HVH = high-voltage heater, HP = heat pump, COP = Coefficient of Performance

Conclusions

Heat pumps represent a promising technical solution for improving the energy efficiency of electric vehicles, particularly under conditions where grid-side preconditioning is not possible. The use of waste heat from vehicle systems can save energy and thereby extend the operating duration of a tractor, provided that sufficient waste heat is available and the temperature of the waste heat medium is high enough to effectively supply the required heat to the heat pump.

In the case of a cold start at 0 °C without preconditioning (with 85% usable battery capacity) as well as a warm start with grid-side preconditioning (100% usable battery capacity), measurements and analyses revealed best values for the Coefficient of Performance (COP) of over 4 at low load. This

results in a machine operating time gain of approximately 7–11% or 14–22 minutes (COP 2–4) in the cold start scenario, and an increase of about 2.6–3.9% or 6–10 minutes in the warm start scenario. The positive effect of heat pumps increases with decreasing machine load, as the heating demand of the cabin remains constant.

Overall, the obtained results underline the potential of heat pumps as a solution to improve energy efficiency and extend the operating time of battery-electric agricultural machinery, especially under real operating conditions without grid-side preconditioning. However, the increased system complexity requires further investigations to comprehensively assess long-term reliability and the resulting impacts on operation.

References

- AGCO GmbH (2026): Fendt e100 Vario | Fendt – Der E-Standardtraktor. <https://www.fendt.com/de/landmaschinen/e-traktoren/fendt-e100vario>, accessed on 27 Jan 2026
- AgroFossilFree (2020): Rigitrac SKE 40 ELECTRIC. <https://www.platform.agrofossilfree.eu/de/view/feft/487>, accessed on 26 Jan 2026
- Breu, W.; Pichlmaier, B. (2017): Electrified Utility Tractor. In: Land.Technik AgEng 2017, VDI Verlag, S. 9–14
- Dohmann, J. (2016): Thermodynamik der Kälteanlagen und Wärmepumpen. Berlin, Heidelberg, Springer Verlag
- Doppelbauer, M. (2025): Grundlagen der Elektromobilität. Wiesbaden, Springer Fachmedien
- Ertel, W. (2025): Grundkurs Künstliche Intelligenz. Wiesbaden, Springer Fachmedien
- Joos, L. (Hg.) (2004): Energieeinsparung in Gebäuden – Stand der Technik, Entwicklungstendenzen. Essen, Vulkan-Verlag
- Korff, L. (2024): Entwicklung einer thermischen Arbeitsmaschine auf Basis des Kaltdampfprozesses mit Sekundärkreislauf für ein elektrifiziertes Fahrzeug. Masterarbeit, FH Münster, unpublished
- Markets and Markets (2025): Electric Tractor Market. <https://www.marketsandmarkets.com/Market-Reports/electric-tractor-market-109801941.html>, accessed on 21 Oct 2025
- Praetorius, B. (2018): Quo vadis Energiewende – Vision und Wirklichkeit. In: In Zukunft elektrisch - Energiesysteme im ländlichen Raum, KTBL-Tage 07.–08.03.2018 in Bayreuth, Darmstadt, KTBL, S. 4–7
- Rigitrac Traktorenbau AG (2025): Rigitrac SKE 40 e-direct Electric. https://www.rigitrac.com/app/download/12054267577/Prospekt+Rigitrac+SKE+40_2025.09_WEB.pdf?t=1768558063, accessed on 27 Jan 2026
- Suck, G.; Spengler, C. (2014): Lösungen für das Wärmemanagement von Batteriefahrzeugen. ATZ – Automobiltechnische Zeitschrift 116(7-8), S. 12–19, <https://doi.org/10.1007/s35148-014-0443-x>
- Weustenfeld, T.A. (2018): Heiz- und Kühlkonzept für ein batterieelektrisches Fahrzeug basierend auf Sekundärkreisläufen. Dissertation, Technische Universität Braunschweig, Cuvillier Verlag, https://leopard.tu-braunschweig.de/servlets/MCRFileNodeServlet/dbbs_derivate_00044210/Diss_Weustenfeld_Thomas.pdf, accessed on 27 Jan 2026

Authors

Benjamin Wilk, M.Sc., is an employee in Electric Drive Technology, **Dipl.-Ing. (FH) Philipp Heymann** is Head of Electric Drive Technology, CLAAS Industrietechnik GmbH, Halberstädter Straße 15-19, 33106 Paderborn and **Dr.-Ing. Jan Wieckhorst** is Head of Tractor Predevelopment, CLAAS Tractor SAS, Paderborn. E-Mail: Benjamin.Wilk@claas.com

Prof. Dr. Ludger Frerichs is Director of the Institute for Mobile Machines and Commercial Vehicles at TU Braunschweig, Langer Kamp 19a, 38106 Braunschweig